

Iterative Highly Constrained Back Projection (HYPR) Reconstruction of Undersampled Diffusion Weighted Data in Hyperpolarized Helium-3 MRI

R. L. O'Halloran¹, J. Holmes¹, E. Peterson², and S. Fain¹

¹Medical Physics, University of Wisconsin, Madison, WI, United States, ²Biomedical Engineering, University of Wisconsin, Madison, WI, United States

Introduction: Apparent Diffusion Coefficient (ADC) imaging with hyperpolarized gas is a useful tool in lung imaging but the commonly implemented 2-point method fails to capture the non-monoexponential behavior of real lung tissue. Diffusion weighting at multiple b-values is desirable to quantify this behavior but is time consuming and difficult in a single breath-hold acquisition. Undersampled projection imaging has been successful [1] in reducing imaging time in HP gas MRI. Because streaks arising from undersampling in standard Filtered Back-Projection (FBP) would impair quantitative analysis of the diffusion data an undersampling-robust image reconstruction is needed for the diffusion images. Highly Constrained Back Projection HYPR [2] uses a nearly fully composite image to deal with the problem of undersampled reconstruction but is non-ideal for non-sparse data sets. Since the images used to create ADC maps are not sparse we have devised an iterative HYPR (I-HYPR) algorithm similar to Ordered Subset Expectation Maximization (OSEM) [3,4]. The algorithm is validated in a simulation and used in reconstructing highly undersampled multi-b-value diffusion data in a human study. The purpose of this work is to show the feasibility of obtaining accurate functional maps in a single breath hold using highly undersampled PR techniques.

Methods: *Algorithm:* The iterative HYPR algorithm was implemented by performing the HYPR reconstruction using subsets of the acquired projections to generate intermediate estimates of the diffusion weighted images. The output of the previous iteration is used as the composite image for the next iteration.

Simulation: Feasibility was tested using simulation data created from a single coronal slice of a human ADC study (60 year old male, 40 pack year smoking history; Fig. 1a). The unweighted data were taken unaltered while the weighted data were radon transformed using 8, 16, 32, and 64 projections. The weighted data was then reconstructed using FBP and I-HYPR and used with the unweighted data to compute ADC maps. The ADC maps were then compared to the ADC map computed with the fully sampled weighted image. I-HYPR reconstruction was done with half as many subsets as projections and 4 iterations using the fully sampled unweighted image as the initial seed image.

Human Study: MRI on a healthy volunteer acquiring 8 b-values ranging from 0.52 to 4.2 s/cm² were acquired in a single 24 s breath-hold over a 3D volume consisting of 10 axial slices at a 3 cm thickness and in-plane resolution of 5 mm² using a fast-GRE 3D PR sequence. Acquisition was performed using a 1.5 T MR scanner (Signa Excite, GE Healthcare, Milwaukee, WI) with a chest coil tuned to the He-3 resonant frequency used to transmit and receive. 16 projections were acquired per b-value followed by 128 projections without diffusion weighting for the fully sampled composite images at each location. The unweighted images were reconstructed with FBP and used as the seed images for I-HYPR reconstruction of the highly undersampled diffusion weighted images. I-HYPR was performed with 8 subsets and 4 iterations.

Results and Discussion: The results of the mean, standard deviation, and entropy calculations in the simulation are presented in Table 1. ADC maps for the cases of 8 and 32 projections in FBP and I-HYPR are shown in Fig. 1. with the ADC map from the fully sampled data at left (Fig. 1a.). At 8 projections the I-HYPR ADC map (Fig 1d) gives an accurate mean but underestimates standard deviation. This effect, likely caused by blurring due to the high level of undersampling, decreases with increasing number of projections as expected. The FBP ADC maps exhibit a high level of streak artifact (Fig. 1b,c). This is, of course, expected as the assumptions inherent to FBP are not met in undersampled data sets. ADC maps from the human study for representative slices and b-values are shown in Fig. 2 demonstrate the regional b-value-dependent diffusivity expected due to differing levels of restriction for alveolar and small airway structures [5].

Conclusion: A method for acquisition and reconstruction of highly undersampled 3D parametric maps of diffusion is presented. This approach makes sophisticated diffusion techniques such as, multi-b-value imaging and diffusion tensor imaging feasible in human lung studies where imaging times are limited to a single breath hold. Future work will focus on validation using quantitative modeling of diffusion coefficients.

References: [1] Wild et al. MRM 2003. [2] Mistretta et al. MRM (2006). [3] Shepp and Vardi. IEEE Trans. Med. Imag. (1982). [4] Erdoğan and Fessler Phys. Med. Biol. (1999). [5] Yablonskiy et al. PNAS (2001).

Acknowledgments: A grant to SBF by the Sandler Program for Asthma Research. GE Healthcare for the loan of the Helium Polarizer.

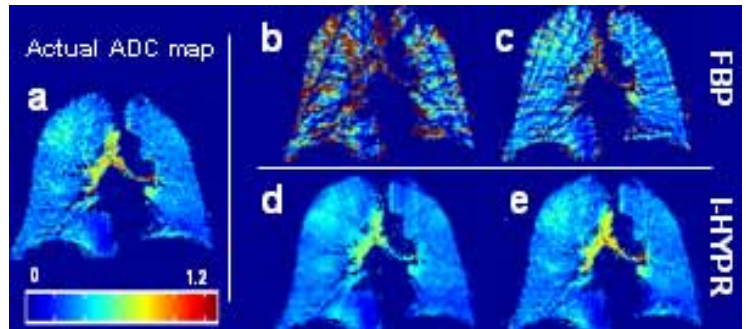


Figure 1: Comparison of ADC maps constructed using I-HYPR and FBP. The ADC map made with the fully sampled data is shown at the top. Colorbar units: cm²/s.

Proj	True			I-HYPR			FBP		
	μ	σ	S	μ	σ	S	μ	σ	S
8	0.35	0.15	2.19	0.34	0.10	2.15	0.51	0.48	1.79
16				0.34	0.12	2.19	0.44	0.44	2.05
32				0.34	0.14	2.20	0.40	0.30	2.17
64				0.34	0.16	2.23	0.38	0.22	2.2

Table 1: Mean (μ), Standard Deviation (σ), and Entropy (S) for I-HYPR and FBP ADC maps.

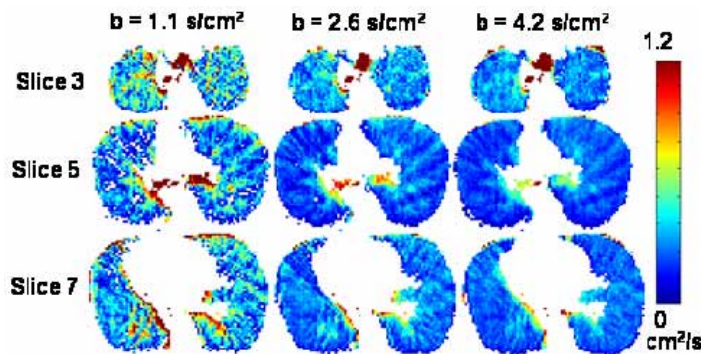


Figure 2: ADC maps from slices 3, 5, and 7 of normal human lungs shown at the three different b-values indicated.